Advances in Engineering Software 175 (2023) 103357

Contents lists available at ScienceDirect

Advances in Engineering Software

journal homepage: www.elsevier.com/locate/advengsoft

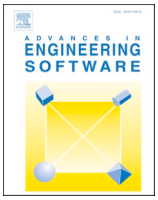

Parametric analysis of railway infrastructure for improved performance and lower life-cycle costs using machine learning techniques

Jose A. Sainz-Aja [a,*], Diego Ferreño [a], Joao Pombo [b,c,d], Isidro A. Carrascal [a], Jose Casado [a], Soraya Diego [a], Jorge Castro [e]

[a] LADICIM (Laboratory of Materials Science and Engineering), University of Cantabria. E.T.S. de Ingenieros de Caminos, Canales y Puertos, Av./Los Castros 44, 39005 Santander, Spain
[b] Institute of Railway Research, School of Computing and Engineering, University of Huddersfield, United Kingdom
[c] IDMEC, Instituto Superior Técnico, Universidade de Lisboa, Lisboa, Portugal
[d] ISEL, Intituto Politecnico de Lisboa, Lisboa, Portugal
[e] Group of Geotechnical Engineering, University of Cantabria. E.T.S. de Ingenieros de Caminos, Canales y Puertos, Av./Los Castros 44, 39005 Santander, Spain

ARTICLE INFO

Keywords:
Railway tracks
Infrastructure assets
Predictive models
Machine learning algorithms
Monte Carlo method

ABSTRACT

Rigorous and efficient management of the railway infrastructure is crucial to avoid accidents and reduce operation and maintenance costs. This requires in-depth knowledge of the assets, the interaction among them and the effect that each track parameter has on the overall infrastructure performance. In this study, a large set of studies are carried out, on a previously calibrated finite element slab track model, where the relevant track parameters are varied within their usual ranges. The results are then used to train and validate a series of predictive models based on Machine Learning algorithms. This methodology provides greater understanding and enhanced prediction of the behaviour of tracks, which are composed of multiple variables such as the soil/subgrade, supporting layers, sleepers, pads and rails. The study also considers train axle loads and service speeds, which are other key elements that influence the track performance. The results show that the parameters that have greatest influence on the railway infrastructure are the properties of the soil, characteristics of the rail pads and the axle loads. This work can support the implementation of predictive maintenance procedures for railway tracks and the development of innovative technological solutions, providing responses to the industrial needs of reducing costs and contributing to improve the competitiveness of railway transport.

1. Introduction

Modern societies require efficient means of transport for passengers and goods. Speed, comfort, safety and environmental friendliness are unavoidable demands nowadays. There are several reasons that have made the railway one of the most used means of transport worldwide. The main advantages of the railway over other alternatives are the high safety level and reliability, together with reduced costs and the low levels of CO_2 emissions [1–3]. According to the Spanish Transport and Logistics Observatory, in 2016, the railway was the means of transport of 28.8% of goods in Spain and more than twice the long-distance journeys were made by train than by airplane [4]. Furthermore, the railway was responsible for 29% of public transport in Spain and the risk of fatal accidents per kilometre is equivalent for railroad and airplane, being 28 times lower than transport by private vehicles [5]. These figures are easily comparably to other countries. According to the European Union, in terms of pollution, in 2014, roads were responsible for 72.8% of total CO_2 emissions in the transport sector, naval was responsible for 13.0% and aviation for 13.1%, while railways only produced 0.6% [6]. Therefore, the use of rail transport helps to reduce dependence on fossil fuels and, at the same time, decrease pollution and carbon emissions that cause global warming.

In order to enhance its advantages and increase its use, the railway sector has undergone a remarkable growth in research, investment and infrastructure development worldwide over the last decades. This evolution in the sector, especially in the case of high-speed rail, has given rise to a large number of studies proposing solutions to improve the mechanical performance and the efficiency of the tracks [7–16]. The accurate characterization of rail infrastructure components has a great importance in vehicle-track interaction studies. Some authors devoted

* Corresponding author.
E-mail address: sainzajaj@unican.es (J.A. Sainz-Aja).

https://doi.org/10.1016/j.advengsoft.2022.103357
Received 1 September 2022; Received in revised form 24 October 2022; Accepted 6 November 2022
Available online 16 November 2022

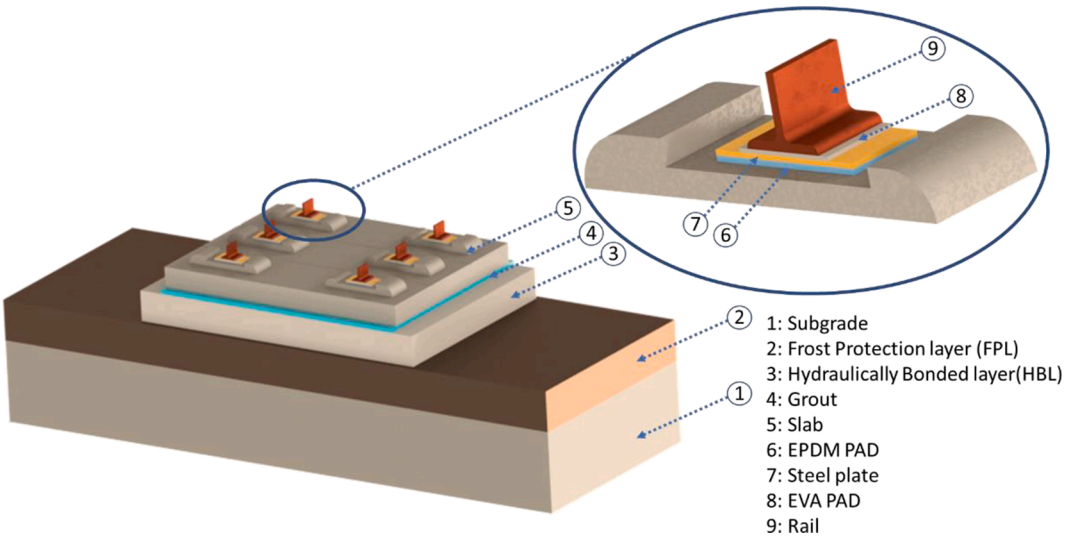

Fig. 1. Elements of the FE track model.

their attention to modelling and characterization of rail pads [17–21], which are the elements with the greatest influence on track stiffness, a fundamental parameter for maintenance of the track [22–27], in particular in the case of ballastless tracks [28–30].

Other authors have proposed co-simulation methodologies using Finite Element Method (FEM) and multibody formulations in order to study the flexibility of track structures under realistic trainset loads [31–34]. These developments open up the possibility of integrating more detailed wheel-rail contact models [35–44], to consider track irregularities [45,46] and other track singularities [10,47–50] in the studies aiming to assess track performance and degradation evolution [51–55] under realistic operation conditions.

Understanding and predicting the behaviour of the track components, their interaction and the influence of load and environmental conditions is of paramount importance for infrastructure managers. Such knowledge enables them to optimize asset management and develop more cost-efficient maintenance procedures, where renewal interventions are defined according to the real conditions of the assets rather than on empirical time intervals.

The large number of variables that affect the performance of railway infrastructure can be categorized into three groups. The weight and speed of the trains are the source of the loads and frequencies acting on the track components. The geographic location of the track is directly related to the environmental conditions, especially the temperature. The response of the system depends on the material properties of the elements that compose the track [56–60] and on the ground that supports it.

To the best of the authors' knowledge, there is currently no study available in the literature aiming to predict the overall response of the track from external actions and the behaviour of its components, including their mutual interaction. The development of computational methods such as FE and Machine Learning (ML) algorithms open up new perspectives in this context. Several recent examples use ML methods to predict the mechanical behaviour of different components. In particular, Kiani et al. [61] develop a series of ML models to predict the structural response and derive fragility curves to assess seismic risk. Kawamura et al. [62] propose an expert rating system for deteriorated concrete bridges based on multilayer neural networks, which takes as inputs just visual inspection and technical specifications. Basudhar et al. [63] establish a methodology for generating decision functions using Support Vector Machine. Ferreño et al. [19] use ML algorithms to generate a series of models to successfully predict the mechanical behaviour of different types of rail pads based on their operating conditions.

The aim of the work presented here is to analyse 4 quantities that are commonly used to assess the dynamic behaviour of the track, namely the displacements and accelerations measured on both the rails and slab. For this purpose, a literature review enabled the identification and classification of the variables influencing the dynamic behaviour of the railway infrastructure. The variables related to the train-induced forces include axle loads, speed, wheel passing frequency and the wheel-rail contact forces. The variable associated with the environment that is considered here is temperature. It is studied in 2 different locations, namely the cities of Seville (Spain) and Moscow (Russia). The material properties of the track components considered comprise the density, Young's modulus and Poisson's ratio of the relevant elements of the fastening system, the concrete slab track characteristics and the geotechnical properties of the soil.

The statistical distributions of infrastructure variables are used to generate synthetic random samples through a Monte Carlo approach [64–66]. In this way, 5400 combination scenarios are defined and simulated using a FE model, which was previously validated experimentally [11,16], in order to obtain the displacements and accelerations of the rail and slab track for each case study. The resulting datasets are then analysed by means of ML algorithms, namely multilinear regression, K-nearest neighbours, decision trees, random forest, gradient-boosting and neural networks (multilayer perceptron). The best model was selected for each of the assessment variables (displacements and accelerations) and interpreted to identify the most relevant features in each case using the permutation importance approach as well as its marginal influence by means of partial dependence plots. This methodology enables the recommended operational ranges for the relevant track features to be established.

The remainder of the paper is organized as follows Section 2.1 defines the FE model as well as the material properties of the track components. Section 2.2 explains the process used to generate the synthetic data, while section 2.3 describes the ML and statistical methods. Section 3 presents the results and their analysis. Finally, section 4 presents the interpretation and relevance of the results obtained.

2. Materials and Methods

2.1. FE Model of the Track

The FE track model used to perform this work is calibrated by laboratory tests [11,16]. This is a dynamic model developed through the Harmonic Response module of ANSYS. To optimise the computational cost, three modifications are made to the original experimentally calibrated model shown in Fig. 1. Firstly, symmetry conditions are applied

Table 1
Dimensions of the track model.

ID	Layer	Material	Width [mm]	Length [mm]	Height [mm]
1	Subgrade + FPL	Compacted sand	6000	2200	1200
3	HBL	Concrete layer (low quality)	3000	2100	300
4	Grout	Bituminous grout	2550	2100	40
5	Slab	Concrete (HA-35)	2550	1930	200
6	Fastening system	EVA / EPDM / TPE	150	160	6
7	Rail (UIC 60)	Steel	–	–	—

so that only one quarter of the original model is used. Secondly, as different types of fastening systems are to be analysed, the three elements that form the fastening in the original model (EPDM elastic PAD, steel plate and rubber pad) are replaced by a single body with mechanical properties equivalent to the three components. Finally, as the two soil layers of the original model, subgrade and frost protection layer (FPL), are both compacted sands, although with different degrees of compaction, it was decided to combine both bodies into a single one with equivalent properties. Fig. 1 shows the final configuration of the system and the different elements involved, whose dimensions are detailed in Table 1.

In order to perform the parametric analysis, synthetic samples are generated from the random selection of values for each of the variables involved. In the following, details of the reference ranges defined in each case are presented.

2.1.1. Soil Properties

The subgrade and the FPL together constitute a compacted sand layer of 1.2 m height. Their behaviour is described by Young's modulus (E), Poisson's ratio (ν), and density (ρ). Average reference values of these properties mat be found, for example, in reference [67], namely, E=250 MPa, $\nu = 0.2$ and $\rho = 1900$ kg/m^3. The authors of references [68–70] propose the use of log-normal distributions for these three properties, with coefficients of variation of 0.30 for E and 0.05 for ν and ρ.

2.1.2. Hydraulically Bonded Layer (HBL)

The HBL is a low-quality concrete layer (C-12/15). According to Eurocode-2 [71], its characteristic compression strength is $f_{ck} = 12$ MPa and mean strength is $f_{cm} = 20$ MPa. The literature [71] suggests that the compressive strength of concrete follows a Gaussian distribution as shown in equation (1). Furthermore, it also provides equation (2), which correlates the compressive strength with the Young's modulus. Combining both expressions, it is possible to generate the statistical distribution of the Young's modulus of concrete C-12/15, a mean value of 27.09 GPa with a standard deviation of 2.33 GPa.

$$\boldsymbol{pdf} = \frac{1}{\boldsymbol{\sigma} * \sqrt{2 * \boldsymbol{\pi}}} * \boldsymbol{e}^{-\frac{(x-\mu)^2}{2*\sigma^2}} \tag{1}$$

$$\boldsymbol{E_c(MPa)} = 22000 * \left(\frac{\boldsymbol{f_c}}{10}\boldsymbol{MPa}\right)^{0.3} \tag{2}$$

Based on Eurocode 2 [71], the Poisson's ratio of HBL is not considered as a statistical variable but as a fixed parameter with a value of 0.20. The database available in reference [72] is used to model the statistical distribution of concrete density as Gaussian, with a mean value of 2445.21 kg/m^3 and a standard deviation of 16.16 kg/m^3.

2.1.3. Grout

Grout is a concrete layer between the slab and the HBL. This element is specific to the slab track typology and its properties are considered fixed for this study, i.e., the ones defined in the calibrated model with E=22.5 GPa, $\nu = 0.2$ and $\rho = 2300$ kg/m^3.

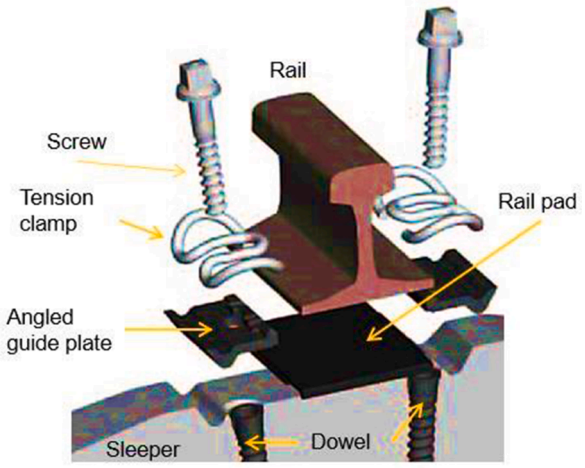

Fig. 2. Fastening system assembly.

Table 2
Train loads applied on the fastening system.

Axle load [ton]	Train Speed [km/h]	Mean Force [kN]	Standard Deviation [kN]
15	120	75.40	1.67
	180	75.40	3.10
	230	75.40	4.97
19	80	93.19	2.63
	130	93.19	1.92
	180	93.19	2.89
22	80	107.90	2.71
	130	107.90	1.96
	180	107.90	2.83

2.1.4. Slab

The slab is made of C-35/45 concrete. The statistical distribution of the properties of this material is obtained in a similar way to the HBL. According to Eurocode 2 [71], the f_{ck} is 35 MPa and the f_{cm} of 43 MPa, resulting in a mean value of 27.09 GPa with a standard deviation of 2.33 GPa. The Poisson's ratio and density are similar to the ones defined for the HBL.

2.2. Elements of the Fastening System

An example of the track fastening system is shown in Fig. 2, showing the elements that compose it. The fastening system is the most variable component of the track assembly. It is made of different materials whose properties depend on operational and environmental conditions such as temperature, train speed, axle load and clamping force of the fastening, also known as 'toe load'. As this is a complex element to simulate, it was decided to replace the entire fastening system with an element with equivalent mechanical properties. To define these properties, the ML algorithm developed by Ferreño et al. is used [19], which provides the dynamic stiffness from the operational conditions. The transformation from stiffness to Young's modulus is done through Young's law. In order to obtain behaviour similar to a spring, Poisson's ratio of this component is fixed at 0 to avoid the effect of contact.

2.2.1. Rail Pad Materials

EPDM, TPE and EVA are the most commonly used materials for rail pads and were considered by Ferreño et al. [19] to generate a regression ML model to predict the dynamic properties of rail pads depending on the operational conditions. The specific literature [73–75] shows that the densities of these materials (mean ± standard deviation) are 1.45 ±0.20, 1.11±0.06 and 0.94±0.01 kg/m^3, respectively. Normal

Table 3
Load frequencies.

Train Speed [km/h]	D_1 [m]	D_2 [m]	f_1 [Hz]	f_2 [Hz]	f_{mean} [Hz]
80	2.70	19.00	1.17	8.23	4.70
120	2.70	19.00	1.75	12.34	7.05
130	2.70	19.00	1.90	13.37	7.63
180	2.70	19.00	2.63	18.52	10.58
230	2.70	19.00	3.36	23.66	13.51

distributions are considered in the 3 cases.

2.2.2. Train Loads

The maximum train-track loads are obtained by computational simulations [76–79] considering conventional railway vehicles with axle loads of 15, 19 and 22 ton. For each axle load configuration, three train speeds are considered as detailed in Table 2. The wheel-rail contact forces are statistically modelled using a Gaussian distribution for each combination of axle load and velocity. In order to transform these forces into load amplitudes supported by the fastening system, it is considered that:

- The fastening system underneath the wheelset supports 50% of the load, it being assumed that the remaining loads are supported by the adjacent sleepers [11,80].
- The load considered is the maximum load, while the minimum is zero, meaning that the amplitude corresponds to 50% of the maximum load.
- A normal distribution is assumed for the application of train loads.

2.2.3. Load Frequency

For each train speed, the distance between wheelsets in the bogies (D_1) and the distance between bogies (D_2) determine the corresponding loading frequencies, f_1 and f_2, as detailed in Table 3. The studies are carried out considering a mean frequency (f_{mean}) between f_1 and f_2.

2.2.4. Temperature

To study the influence of environmental temperature, two locations with different thermal profiles were considered, Seville (Spain), as an example of a very hot city, and Moscow (Russia), as a very cold city. In the case of Seville, the maximum daily temperature throughout the year is considered and in Moscow the minimum daily temperature [81,82] is considered. These datasets enable the empirical Cumulative Distribution Functions (CDF), shown in Fig. 3, to be developed.

2.2.5. Clamping/Toe Load

The connection between the rail and the sleeper is achieved by means of a pair of bolts that compose the fastening system. When tightened, these bolts compress the metal clips and the pads, fixing the rail to the sleeper, as depicted in Fig. 2. According to the literature [18], the nominal value of the tightening force on the bolt is 18 kN. The tightening intensity is determined by the torque supplied to the bolt. However, it is neither immediate nor easy to estimate the compressive force on the rail pad because of the frictional forces during tightening, which are influenced by the usual presence of dust, sand or grease, which reduce the net value of compression. Despite being an important parameter, since it introduces a constant stress state on the rail pad, no record of its value was found in the literature. For this reason, the following four scenarios (previously defined by Sainz-Aja et al. [18]) were considered:

- $F_{toe\text{-}load} = 1$ kN: Represents the possibility that the fastener is broken or loose and therefore does not exert any clamping force.
- $F_{toe\text{-}load} = 9$ kN: Represents the possibility that the fastening has not reached the nominal tightening value.
- $F_{toe\text{-}load} = 18$ kN: Nominal tightening value based on literature.
- $F_{toe\text{-}load} = 25$ kN: Represents the possibility that the fastening has been over-tightened.

2.2.6. Rail

The rail properties were considered to be deterministic because EN 13674-1 [83] specifies conditions in the selection of materials and in the manufacturing process of rails that minimise the possible dispersion of their properties. Here, it is considered that E=200 GPa, $\nu = 0.2$ and $\rho = 7800$ kg/m^3.

2.3. Generation of Synthetic Samples

A total of 5400 random samples were generated using the Monte Carlo method [64–66] corresponding to specific operating conditions. These samples define the 5400 scenarios that were subsequently studied using the track FE model in order to obtain the respective displacements

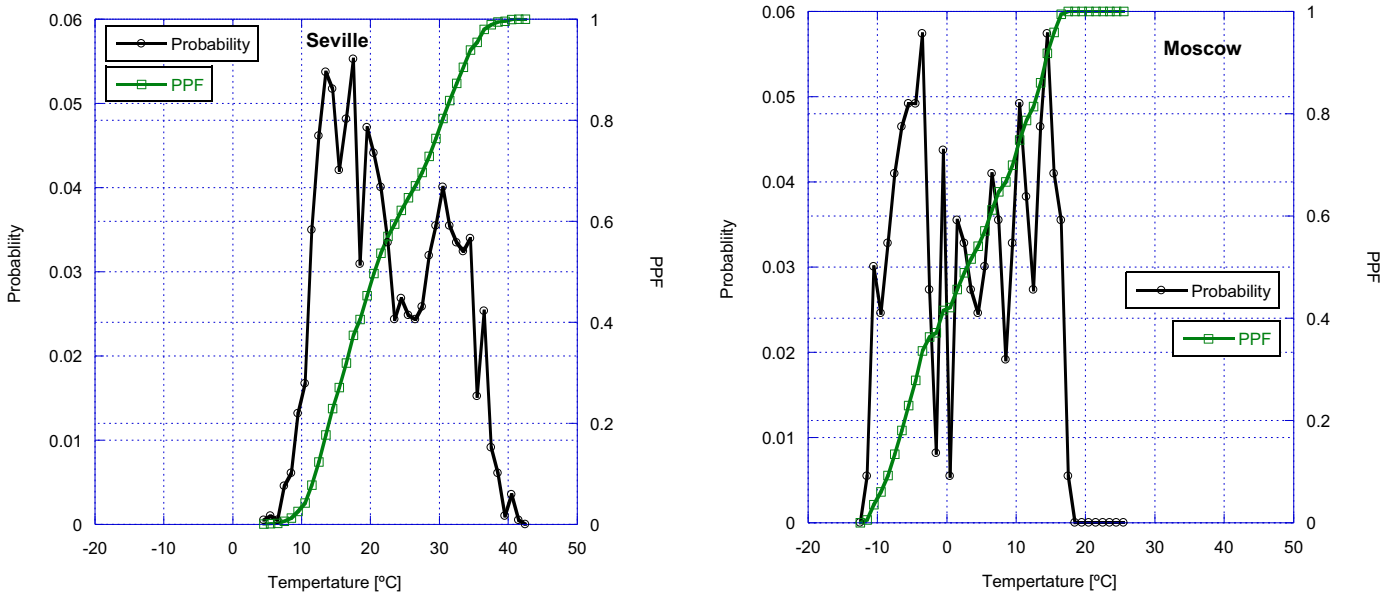

Fig. 3. Temperature statistical distribution in Seville and Moscow.

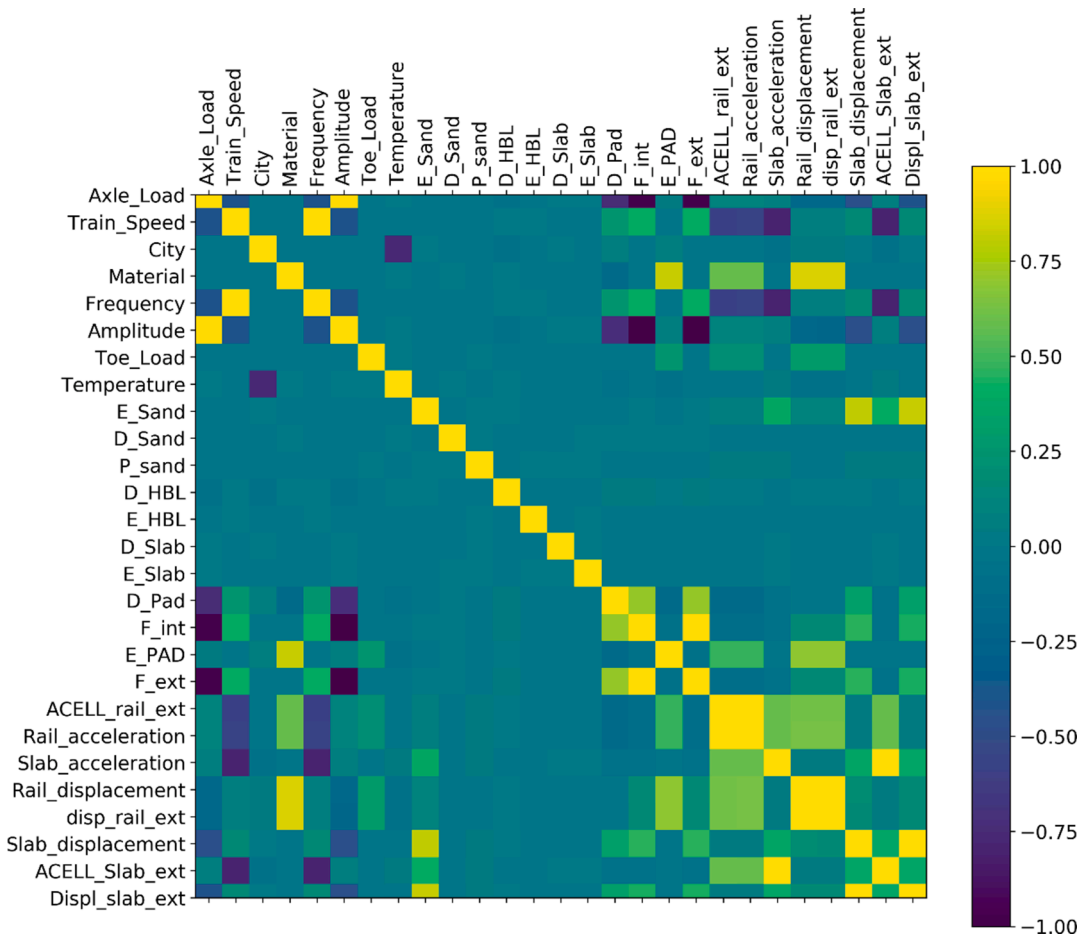

Fig. 4. Correlation matrix.

and accelerations.

2.4. ML Algorithms

The dataset used to perform the analysis by means of ML algorithms consists of 5400 samples, each of them includes 27 features. These 27 features comprise 19 inputs and 8 outputs. The 19 inputs can be organised in two categories:

- Train type-specific variables: train axle load (Train_axle_load), train speed (train_speed), frequency of wheel passing (frequency), load amplitude supported by the rail fastening (amplitude), force applied on the inner FE fastening (Fint) and the force applied on the outer FE fastening (Fext).
- Variables dependent on track location: city (City), rail pad material (Material), toe load (Toe_Load), city temperature (Temperature), modulus of elasticity of: sand (E_sand), HBL (E_HBL), slab (E_slab) and rail pad (E_PAD); density of: sand (D_sand), HBL (D_HBL), slab (D_slab) and seat plate (D_PAD) and; Poisson's ratio of sand (P_sand), HBL (P_HBL) and slab (P_slab).

The mechanical behaviour of the slab track is defined based on eight outputs. These correspond to the acceleration and vertical displacement of four key points of the track model, namely the railhead and the sleeper of the two modelled segments.

- Outputs: Acceleration in external rail of the model (ACELL_rail_ext), acceleration in internal rail of the model (ACELL_rail_int), acceleration in external slab of the model (ACELL_slab_ext), acceleration in internal slab of the model (ACELL_slab_int), displacement in external rail of the model (dis_rail_ext), displacement in internal rail of the model (dis_rail_int), displacement in external slab of the model (dis_slab_ext) and displacement in internal slab of the model (dis_slab_int).

To perform the analysis of the dataset, the first step is to standardise all the data using the StandardScaler algorithm available in the Scikit-Learn python library. Subsequently, the dataset is randomly divided in 4049 instances for training (75 % of instances) and 1350 instances for testing (25% of the instances).

Six ML algorithms available in the Scikit-Learn library are used for regression modelling, these are described below. To evaluate the quality of the regression models, four different parameters were analyzed: R2, RMSE (Root-mean-square-error), MAE (Mean-absolute-error), and MAPE (mean-absolute-percentage-error).

- Logistic regression (LR) [84]: LR measures the relationship between the dependent variable and the independent variables using the sigmoid/logistic function.
- K-Nearest Neighbors (KNN) [85]: this algorithm conducted for a new observation by analyzing the output variable of the "K" closest observations.
- Decision Tree (DT) [86]: is a non-parametric supervised learning method used for classification and regression.
- Random forest (RF) [87]: combine multiple "weak classifiers" (decision tree) into a single "strong classifier".

Table 4
Feature correlation higher than 0.75.

Feature 1	Feature 2	|r|	Feature 1	Feature 2	|r|
Amplitude	F_int	1	Material	disp_rail_ext	0.87
Amplitude	F_ext	1	Material	Rail_displacement	0.87
F_int	F_ext	1	Material	E_PAD	0.82
Train_Speed	Frequency	1	E_Sand	Displ_slab_ext	0.82
Rail_displacement	disp_rail_ext	1	E_Sand	Slab_displacement	0.82
ACELL_rail_ext	Rail_acceleration	1	Train_Speed	Slab_acceleration	0.78
Slab_displacement	Displ_slab_ext	1	Frequency	Slab_acceleration	0.78
Slab_acceleration	ACELL_Slab_ext	1	Train_Speed	ACELL_Slab_ext	0.78
Axle_Load	Amplitude	0.98	Frequency	ACELL_Slab_ext	0.78
Axle_Load	F_int	0.98	City	Temperature	0.75
Axle_Load	F_ext	0.98			

Table 5
Features replacement.

Saved variables	Replaced variables
Amplitude	Axle_load, F_int, F_ext
Train_Speed	Frequency
Temperature	City
E_PAD	Material

- Gradient Boosting (GB): is a machine learning technique used for regression problems, which produces a predictive model in the form of an ensemble of weak prediction models.
- Multi-Layer Perceptron (MLP) [88]: is an artificial neural network composed of multiple layers.

One of the great features of ML algorithms is that they can evaluate and compare the correlation of each variable with the predicted outcome. In this work, two different algorithms are used to estimate feature importance, namely, impurity-based and permutation-based ones, both integrated in the Scikit-Learn library [89,90].

To evaluate the effect of each variable within the range of parameters analysed, Partial Dependence Plots (PDPs) are used, which is a tool that enables the analysis of the influence of each variable on the value predicted by the algorithm previously calibrated according to the value that the variable takes.

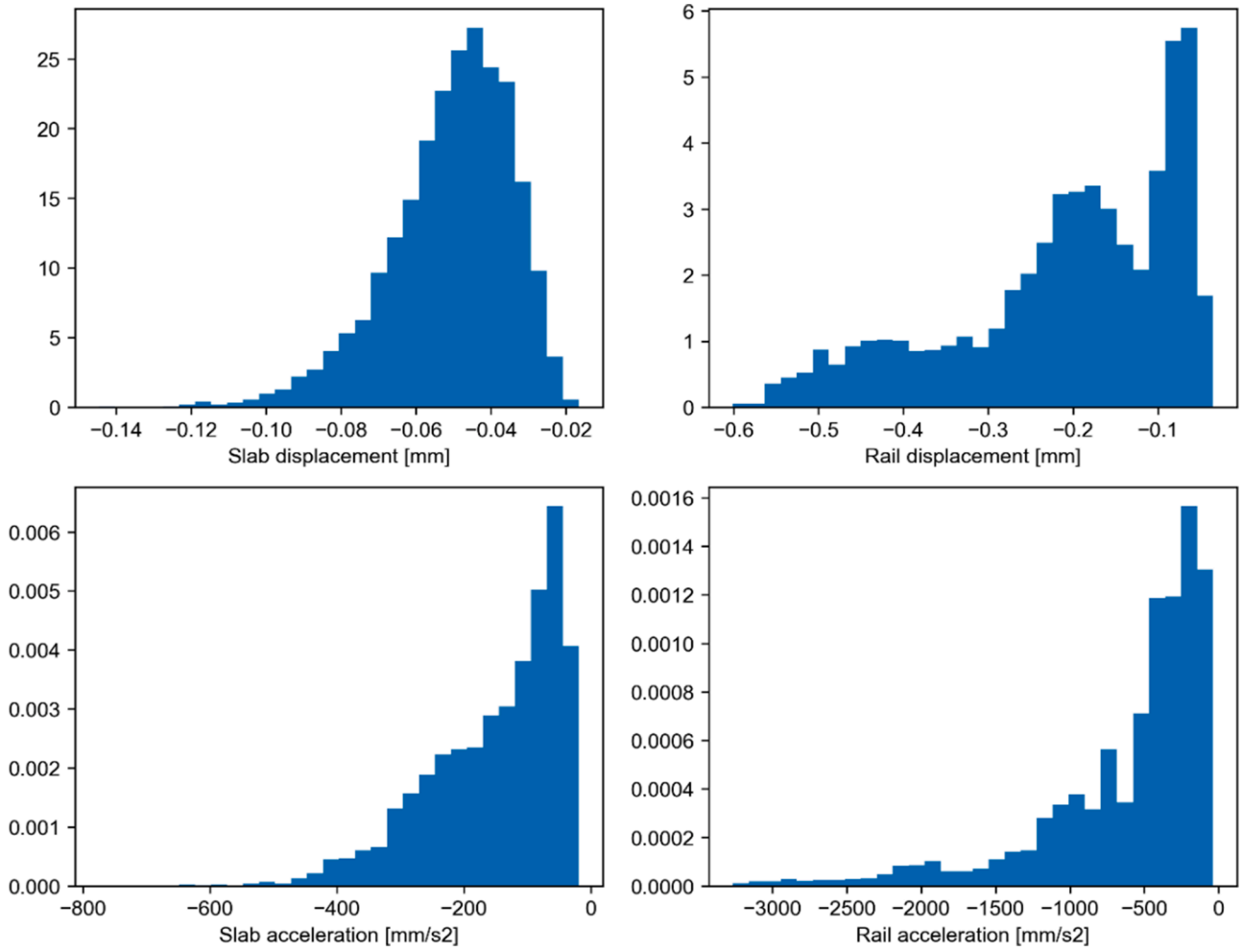

Fig. 5. Output distribution.

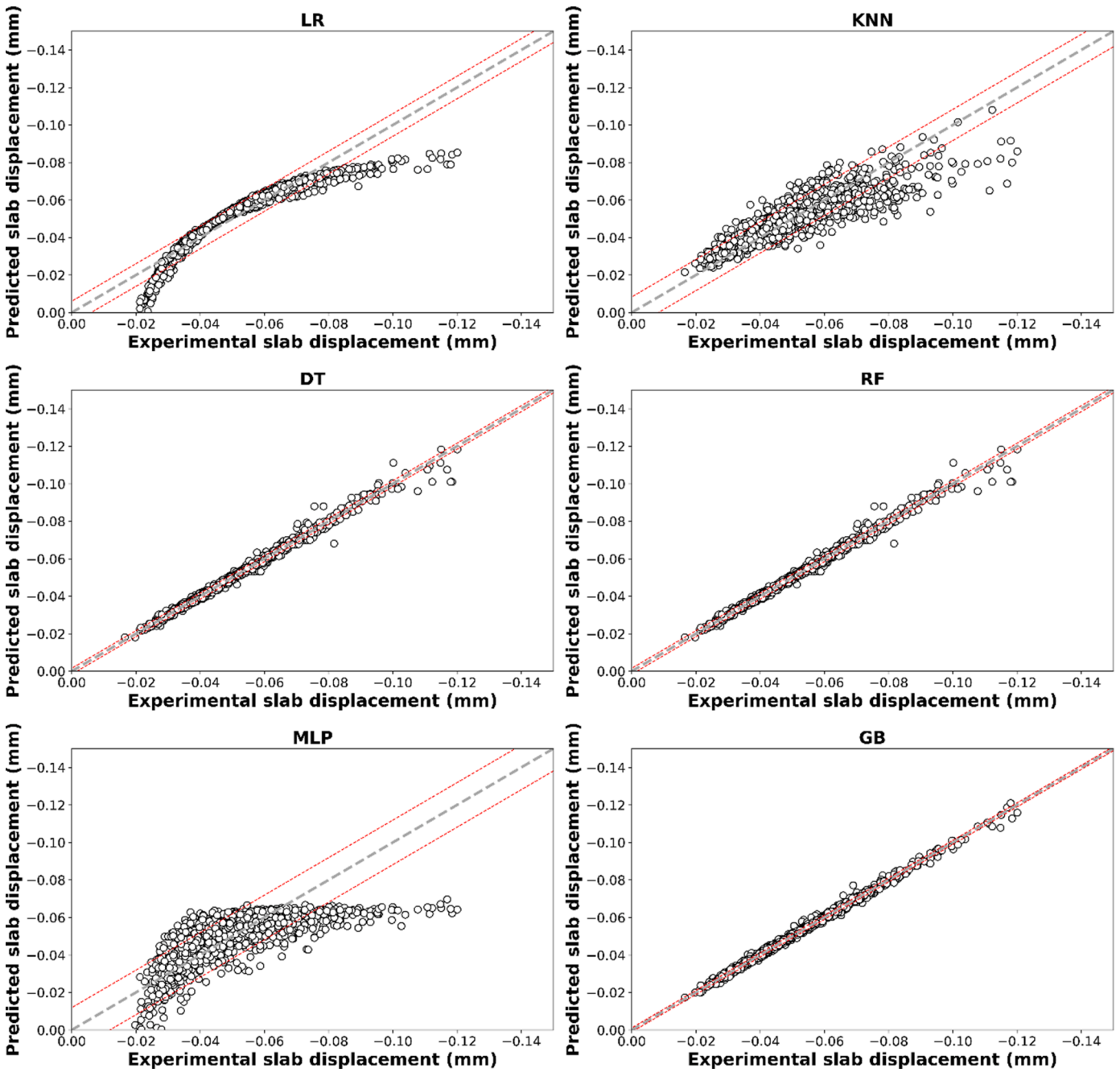

Fig. 6. Algorithm optimization for case study 1 (slab displacement).

3. Results

3.1. Exploratory Data Analysis

Firstly, as there is such a large number of variables and being aware that there is a correlation among several of them, a feature correlation analysis was carried out to analyse whether there was a linear correlation between variables, see Fig. 4. Table 4 shows the correlation values between pairs of variables greater than 0.75. Based on the results obtained in this correlation matrix, a number of variables were eliminated as detailed in Table 5. This preliminary analysis also enabled the verification that the results for both displacements and accelerations in the inner and outer parts were comparable, so, from now on, only inner values will be considered. This first analysis also showed that there is a strong correlation between the rail displacement values and the materials used to manufacture the bedplates, and between the speed of the trains and the accelerations recorded.

As a general analysis of the dataset, a histogram of the outputs available in the model is drawn, as shown in Fig. 5.

3.2. Optimization of the Algorithms for Regression

From this point onwards, 4 different regression models will be used, one for each output available in the model. Case 1 corresponds to slab displacement, case 2 to rail displacement, case 3 to slab acceleration and case 4 to rail acceleration. Fig. 6, Fig. 7, Fig. 8 and Fig. 9 show a comparison between the values obtained experimentally and those provided by each model in the test data, i.e., in those cases that have not been used to calibrate the model. Table 6 shows the quantitative parameters that enable the estimation of the quality of the model. From the data shown

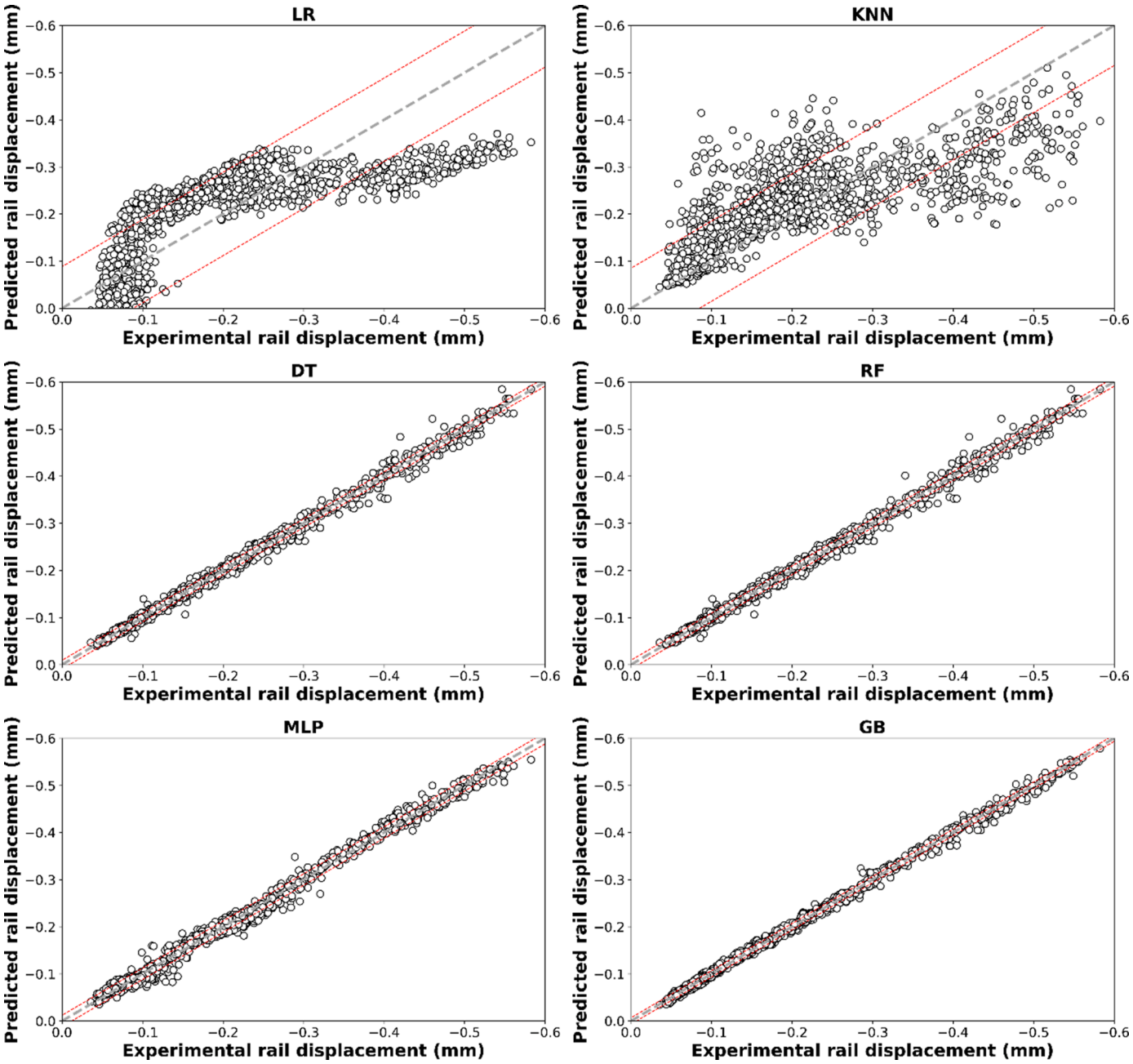

Fig. 7. Algorithm optimization for case study 2 (rail displacement).

in these figures and the table, it is possible to conclude that the decision tree (DT), random forest (RF) and gradient boosting (GB) models are the best fitting models, providing models of similar quality.

The results obtained when evaluating the quality of the predictive models considered here show that, in all case studies, the RF exhibits an R2 higher than 0.979 and a MAPE lower than 6.23%. This reveals that RF has the greatest predictive capacity. Therefore, in the following, only the RF model is considered and the analyses continue in order to extract more information from the track model. In particular, two types of analysis are carried out. Firstly, the variables with the greatest influence on each of the parameters analysed are identified. Then, the influence of these main variables throughout the study range is investigated.

3.3. Feature Importance

Fig. 10 shows the results of the impurity-based and the permutation-based methods, which are indicators of the weight that each variable has in the results. It can be seen that, in each case study, the variables that both methods indicate as most relevant are similar. The only appreciable difference is that in case study 2, the variables Toe_Load and Amplitude, which have similar influence values in the two methods, are in reverse order.

From these results, it can be concluded that the parameters governing the behaviour of the slab and rail head are the same in the case of displacements and accelerations if the variable Train_speed is added. With regard to the behaviour of the slab, the parameters that have the greatest influence are mainly E_sand and Amplitude. In the case of rail head behaviour, the parameters that have the greatest influence are E_pad, Amplitude and Toe_Load.

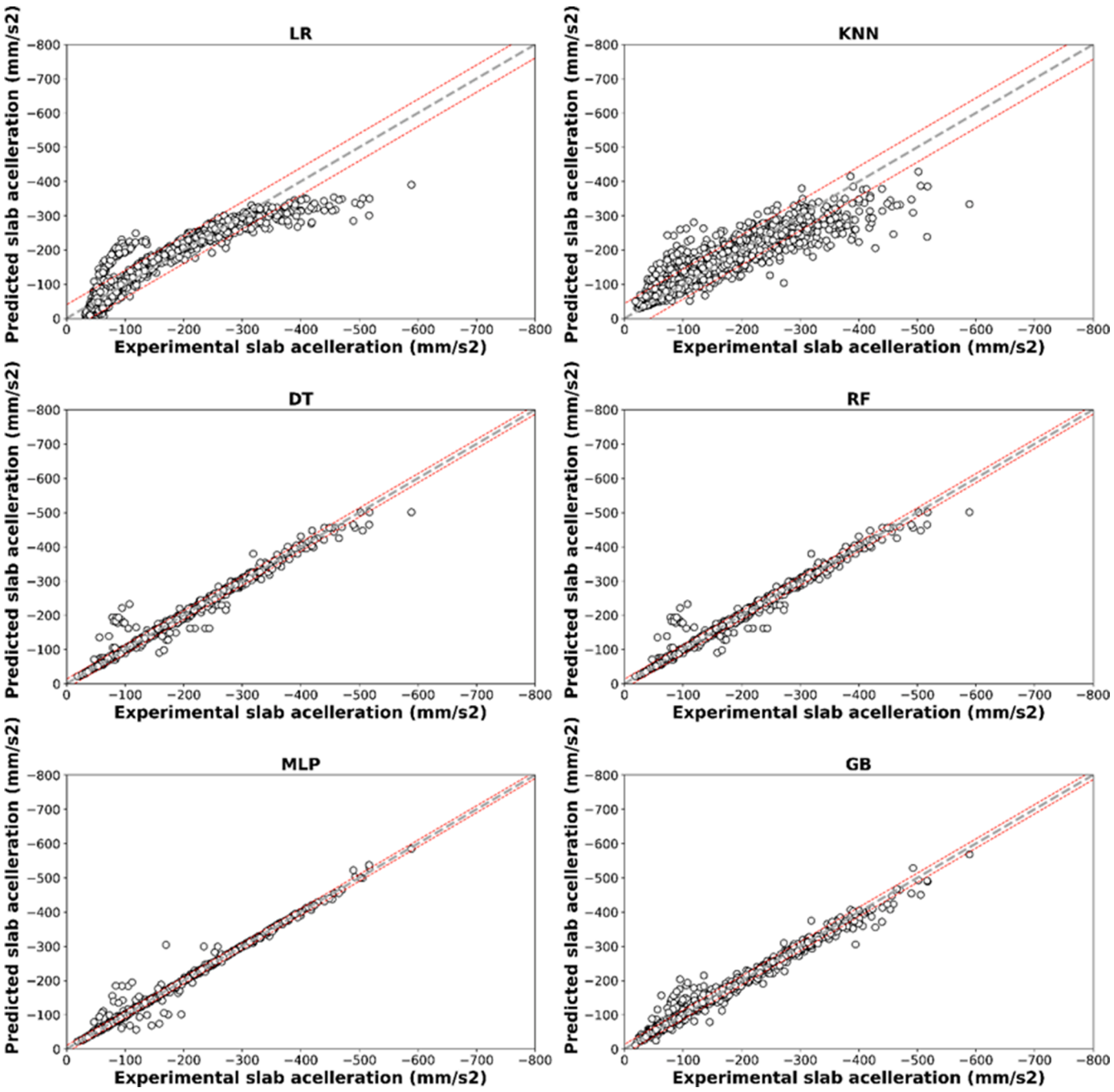

Fig. 8. Algorithm optimization for case study 3 (slab acceleration).

3.4. Partial Dependence Plots

Fig. 11 to Fig. 14 show the PDPs for each case study for the variables that were defined as the most relevant in the previous section. From Fig. 11, it can be seen that as E_Sand increases, the vertical displacement of the slab decreases. On the other hand, the greater the amplitude, the greater the displacement of the slab. It should be remembered that the sign criterion of the FEM implies that larger displacements mean more negative values. It can also be observed that the degree to which E_Sand influences is notably greater than that of Amplitude, as can be seen in the previous section.

Fig. 12 shows the effect of E_PAD, Amplitude, Toe_Load and E_Sand on the vertical displacement of the rail. In the case of E_PAD, it can be seen that the lower the E_PAD, the greater the vertical displacement of the rail, especially in those cases where the E_PAD is less than 100 kN/mm. In the case of Amplitude, it can be seen that the higher the Ampliutde, the greater the vertical displacements in the rail, with an approximately uniform evolution throughout the range studied. In the case of the Toe_Load there is also an approximately constant distribution over the range studied, with vertical displacements increasing as the Toe_Load is reduced. Finally, in the case of E_Sand, it can be seen that the effect is quite similar to that of a variation in E_PAD, but with notably lower values (up to 0.1 in the case of E_Sand and up to 0.5 in the case of E_PAD).

Fig. 13 shows the effect of Train_Speed, Amplitude, E_Sand and Temperature on the accelerations measured in the slab. Regarding speed, it is observed that the higher the speed, the higher the acceleration values recorded. In the case of Amplitude, a similar effect can be

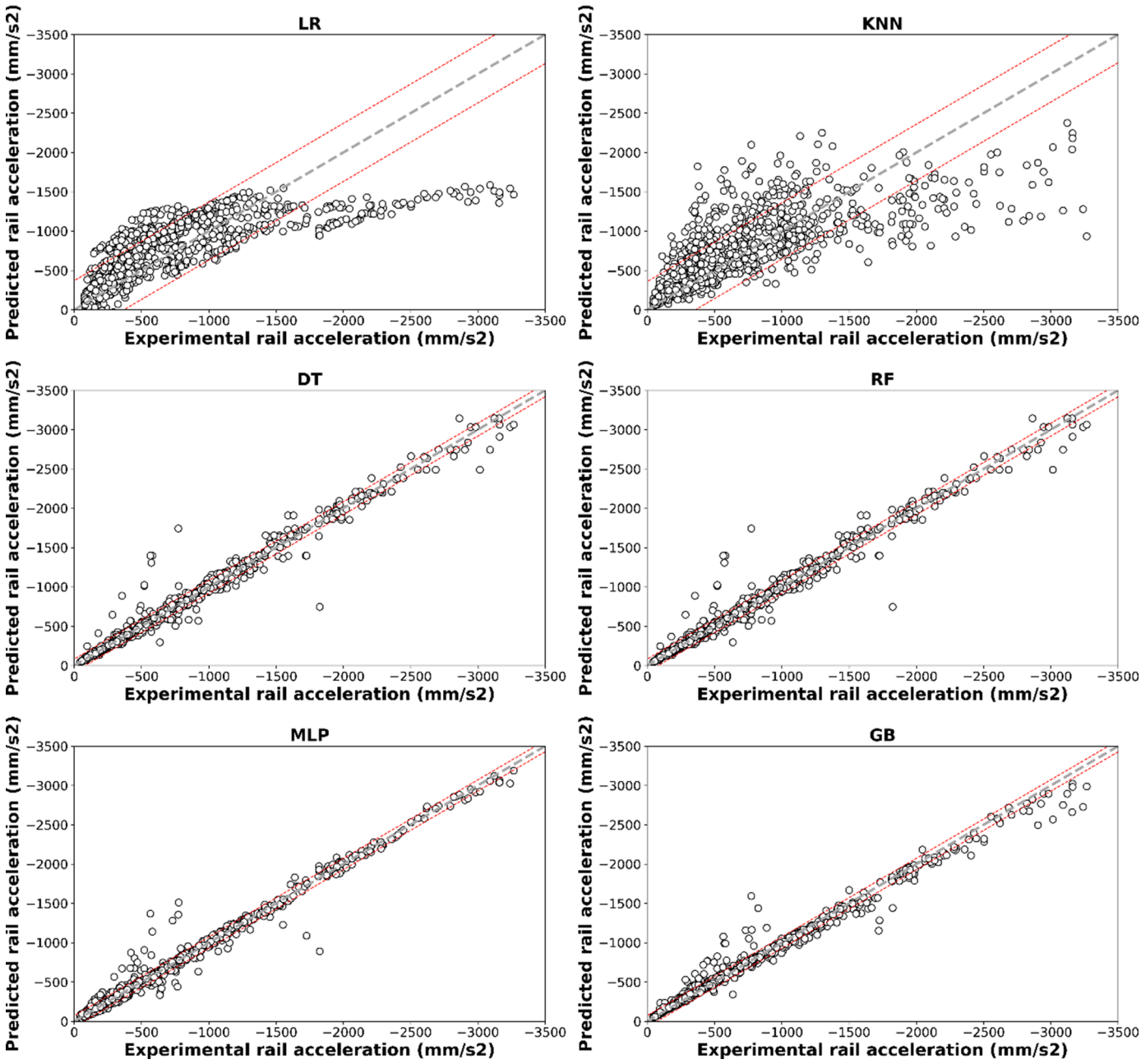

Fig. 9. Algorithm optimization for case study 4 (rail acceleration).

Table 6
Model quality parameters in testing data.

ML Method	Case Study 1		Case Study 2		Case Study 3		Case Study 4	
	R2	MAPE	R2	MAPE	R2	MAPE	R2	MAPE
LR	0.865	-9.07	0.542	-48.11	0.847	-31.24	0.580	-87.87
KNN	0.744	-11.71	0.575	-35.06	0.807	-25.39	0.605	-47.47
DT	0.991	-1.73	0.995	-3.35	0.983	-3.78	0.979	-6.22
RF	0.991	-1.72	0.995	-3.37	0.983	-3.79	0.979	-6.23
MLP	0.476	-18.80	0.991	-6.25	0.990	-2.85	0.984	-8.50
GB	0.996	-1.55	0.997	-2.94	0.982	-6.58	0.984	-7.42

observed, i.e., increasing Amplitude leads to higher accelerations. The effect of E_sand is similar to that seen in the case of slab displacements, but influencing to a lesser degree. Finally, in the case of temperature, it can be seen that the influence is minimal, an observation that is consistent with the results obtained in the previous section.

Fig. 14 shows the effect of E_pad, Amplitude, Train_Speed and Temperature on the measured accelerations on the rail. It can be seen that E_PAD is not only the parameter that has the greatest effect, as in the case of rail displacement, it also has a similar effect to that seen in the case of rail displacement. In the case of the amplitude, it can be seen that

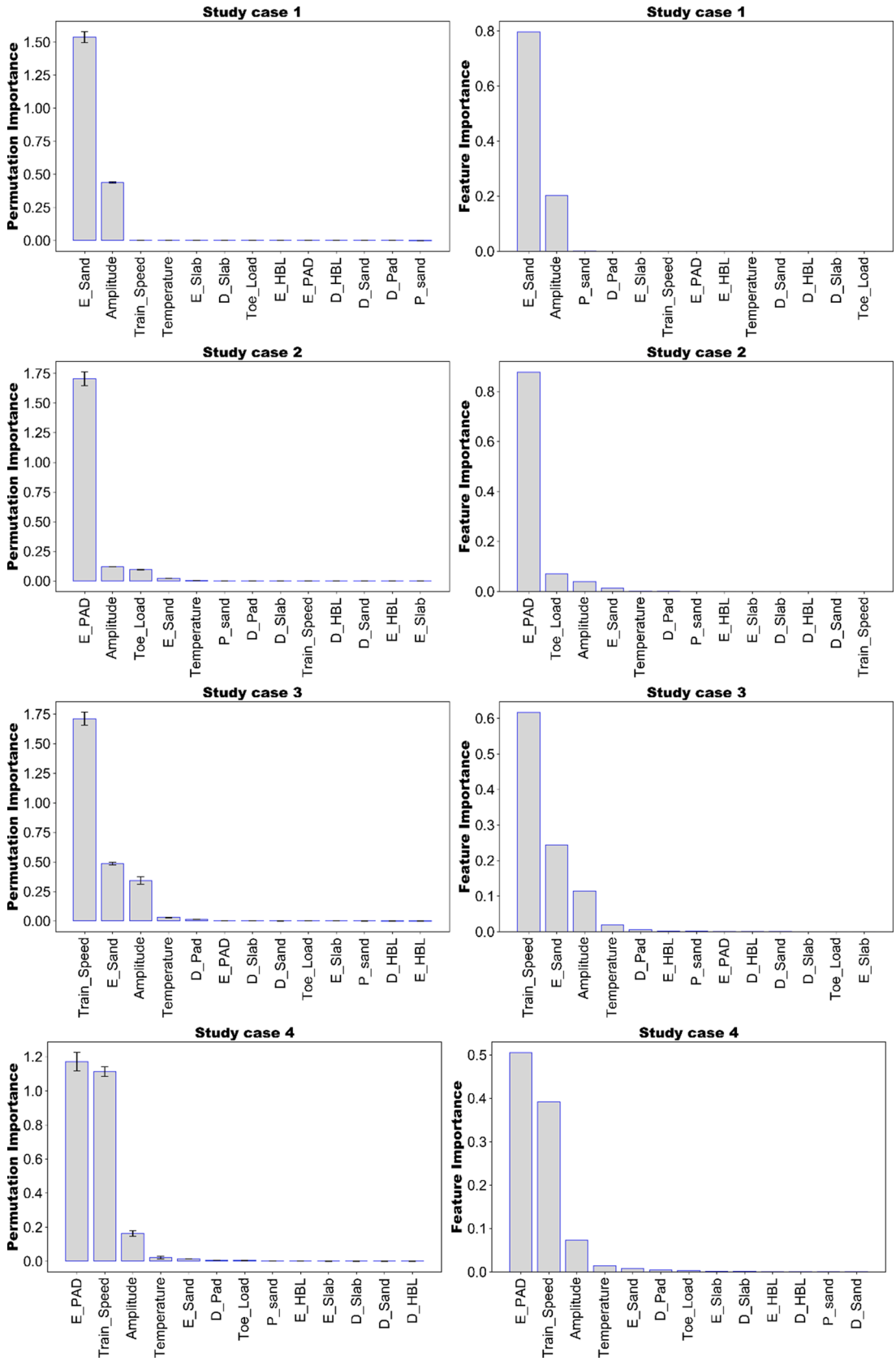

Fig. 10. Permutation importance and feature importance for the 4 case studies.

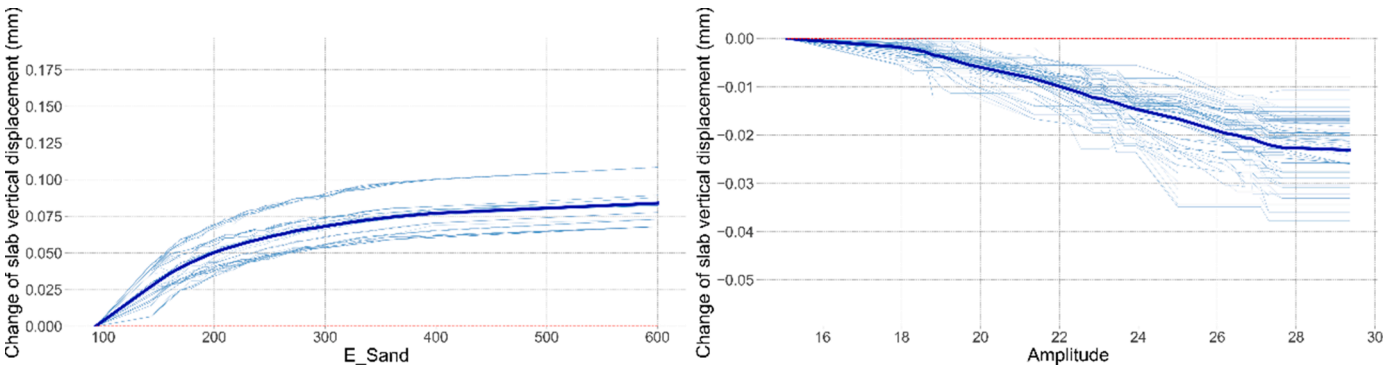

Fig. 11. PDP for relevance variables in case study 1 (slab displacement).

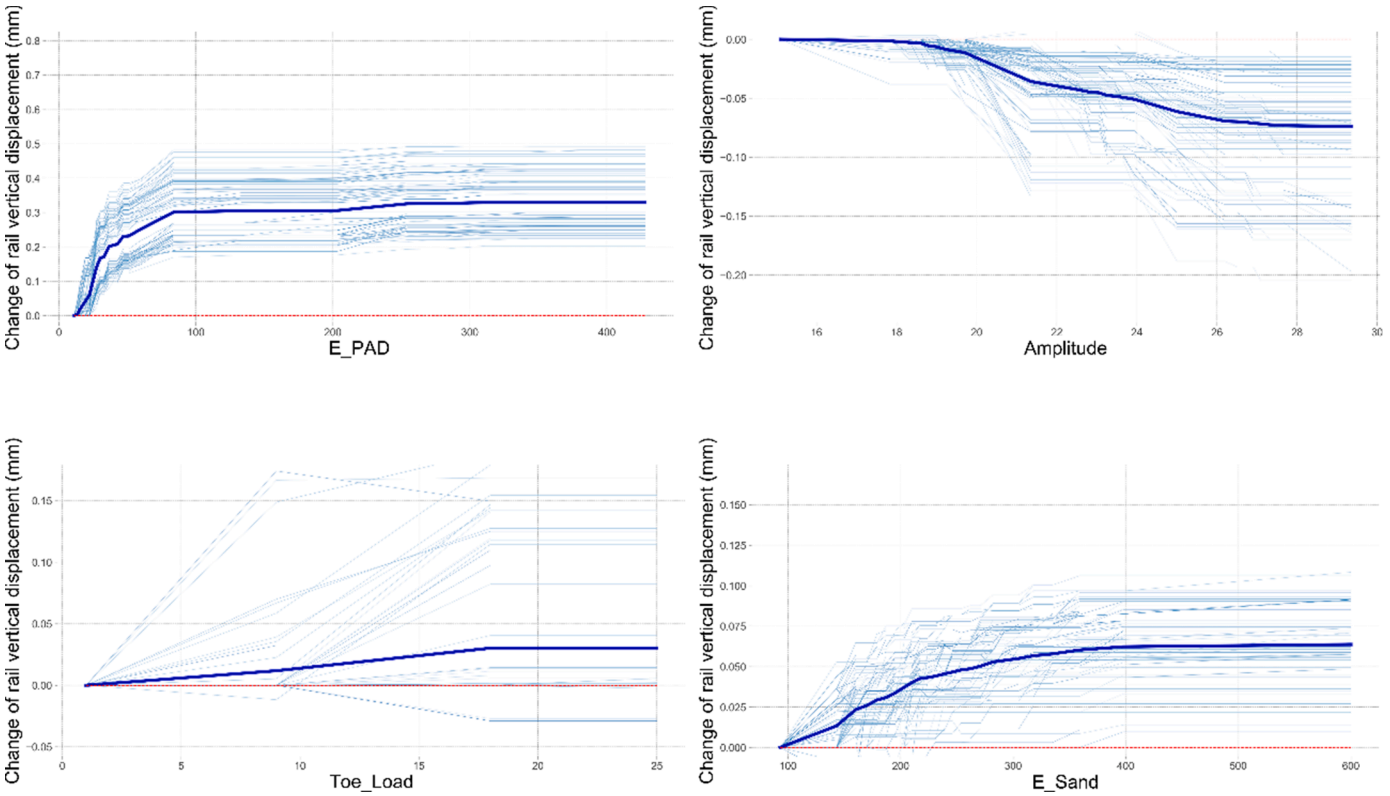

Fig. 12. PDP for relevance variables in case study 2 (rail displacement).

the greater the amplitude is, the greater are the accelerations on the rail. In the case of Train_Speed, it can be seen that it has an approximately linear effect on the acceleration in the rail and that the higher the Train_Speed, the higher the accelerations. Regarding Temperature, it is observed that it has hardly any influence on the rail acceleration.

Previously, the variables were classified into those that are specific to the location of the track and those that are dependent of the train running on the track. When analysing these last two sections according to this classification, it can be noticed that regarding the variables that are dependent on the location of the track, in the case of focusing on the slab, the main parameter to take into account would be the E_sand, with all the others being several orders of importance below it. If the focus is on the behaviour of the rail, it is observed that the most important parameter is the E_PAD but that E_sand and Toe_Load also have a certain degree of influence. On the other hand, regarding the variables that depend on the train running on the track, it is demonstrated that Amplitude, directly related to the train axle load, is a parameter that, although in no case is it the most important one, in all cases has significant importance. The results also reveal that Train_Speed has a great repercussion in the case that the parameter to be analysed is the acceleration.

3.5. Data Correlation with Principal Variables

To conclude the analysis, a correlation is sought between the experimentally obtained values and the variables identified as critical. Fig. 15 demonstrates how the crucial variables have clearly marked patterns in the distribution of the results.

4. Conclusion

In this work, a total of 5400 simulations of a previously calibrated FE track model were carried out, modifying each of its 27 features within their usual variation ranges. Based on these results, a number of machine learning predictive algorithms were trained and validated. This methodology provided deeper understanding of complex track systems,

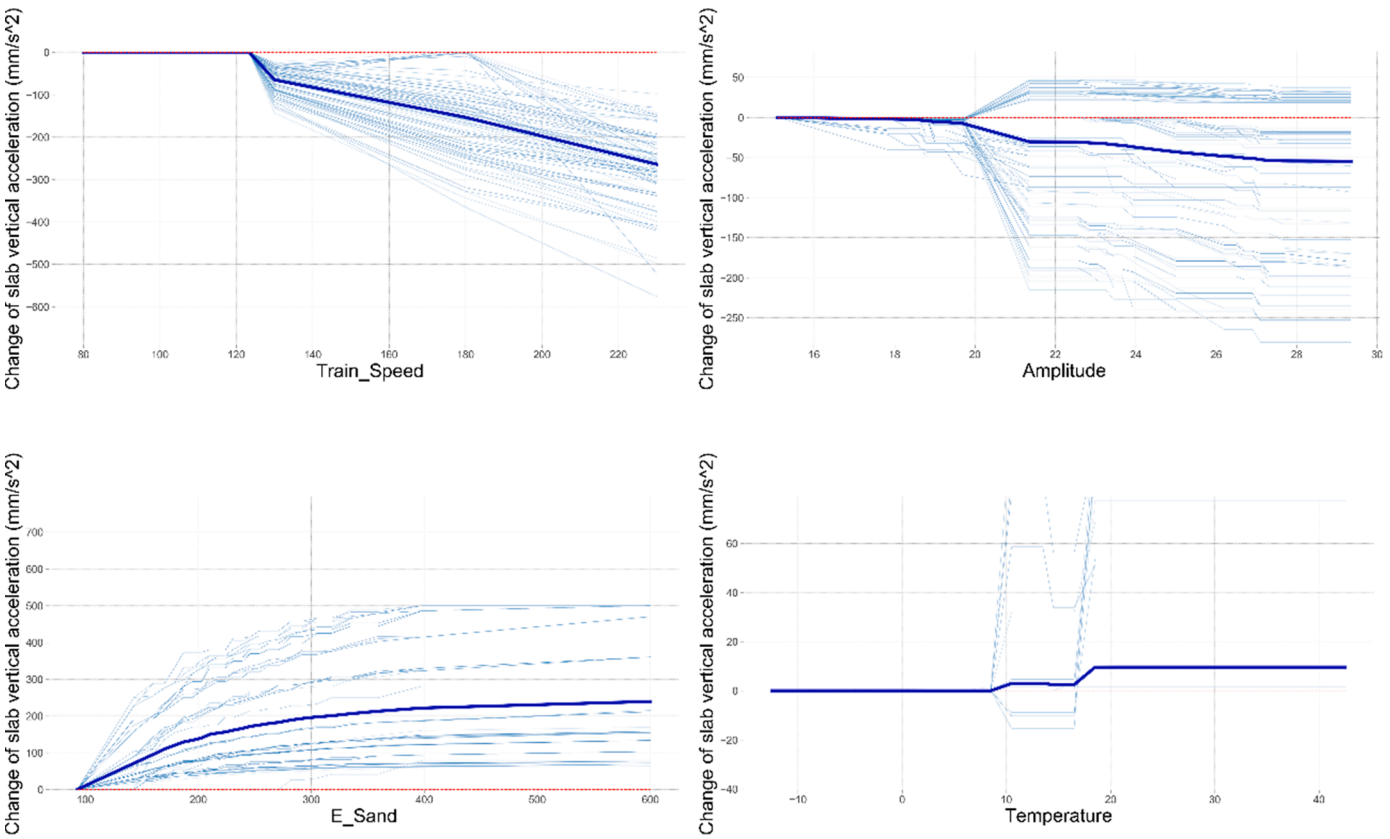

Fig. 13. PDP for relevance variables in case study 3 (slab acceleration).

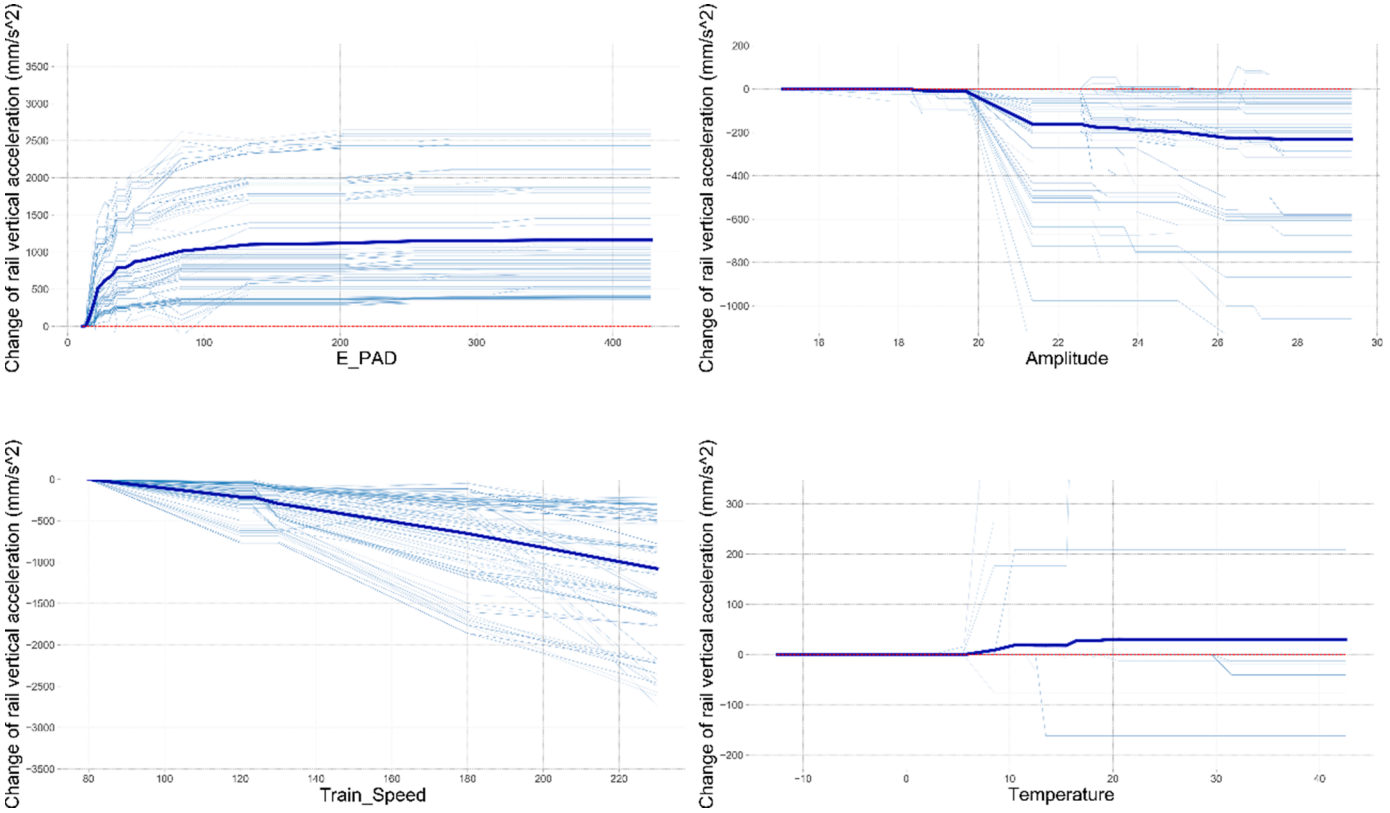

Fig. 14. PDP for relevance variables in case study 4 (rail acceleration).

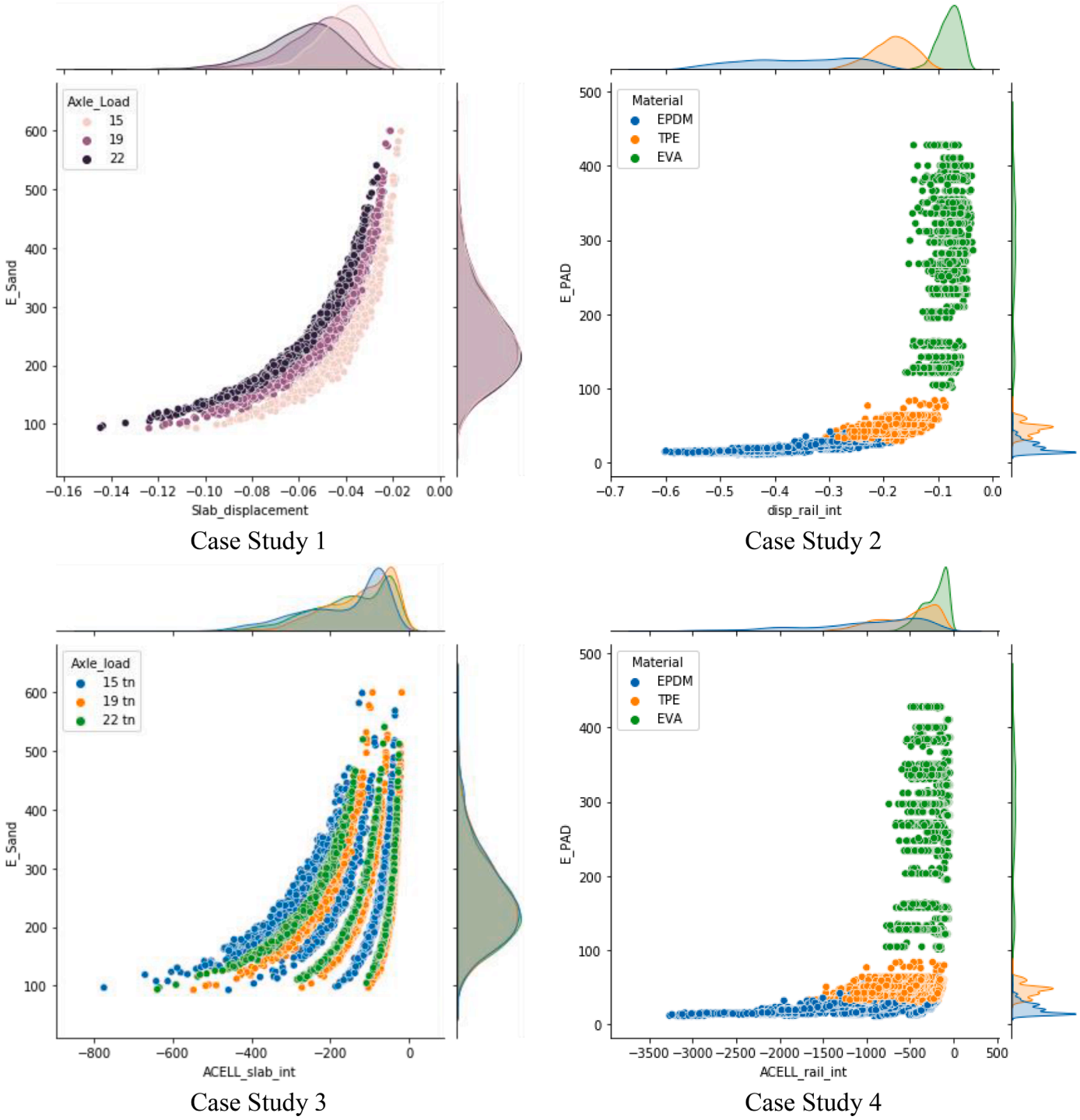

Fig. 15. Correlation of each output with the most relevant variables.

aiming to identify the parameters that have most influence on the track performance and to plan the maintenance interventions based on the real conditions of the critical assets. These studies enabled the following conclusions to be drawn:

- Seven predictive models were calibrated, the best of all being the RF (Random Forest) with an R^2 always greater than 0.979 and a MAPE lower than 6.23%.
- The parameters with the greatest influence on the vertical displacements of the slab are E_Sand and Axle load.
- The quantities with the greatest influence on the vertical displacements of the rail are E_PAD, Toe_load, Axle load and E_sand.
- The parameters with the greatest influence on the vertical accelerations of the slab are Train_Speed, Axle load and E_Sand.
- The parameters with the greatest influence on the vertical accelerations of the rail are E_PAD, Axle_Load and Train_Speed.
- The influence of E_sand and E_PAD are greater when they are lower.

The results obtained here provide valuable information in terms of identifying the track features and operation conditions that are most relevant when designing a new railway track or when defining specific

predictive maintenance strategies. Another important outcome of this work is the identification of the parameters that should be modified/ adjusted in the event that problems are observed during the operation of an existing section of track.

Funding

The authors would like to thank the MCIN/AEI/ 10.13039/ FEDER, UE for financing the project Pry PID2021-128031OB-I00 "Development of a System to Monitor Automatically High- Speed Railway Lines Through Machine Learning and Numerical Simulation Algorithms (SMART- Algorithms).

CRediT authorship contribution statement

Jose A. Sainz-Aja: Conceptualization, Methodology, Software, Formal analysis, Investigation, Data curation, Writing – original draft. **Diego Ferreño:** Conceptualization, Formal analysis, Writing – original draft, Software, Writing – review & editing, Supervision. **Joao Pombo:** Conceptualization, Formal analysis, Writing – review & editing. **Isidro A. Carrascal:** Conceptualization, Methodology, Formal analysis, Writing – review & editing, Supervision. **Jose Casado:** Conceptualization, Formal analysis, Writing – review & editing. **Soraya Diego:** Resources, Investigation, Data curation. **Jorge Castro:** Methodology, Formal analysis, Data curation.

Declaration of Competing Interest

The authors declare that they have no known competing financial interests or personal relationships that could have appeared to influence the work reported in this paper.

Data Availability

Data will be made available on request.

Acknowledgments

The authors would like to thank: LADICIM, the Laboratory of Materials Science and Engineering of the University of Cantabria, for making the facilities used in this research available to the authors. The contribution of J. Pombo to this work was supported by FCT, through IDMEC, under LAETA, project UIDB/50022/2020.

References

[1] He G, Mol APJ, Zhang L, Lu Y. Environmental risks of high-speed railway in China: Public participation, perception and trust. Environ Dev 2015;14:37–52. https://doi.org/10.1016/j.envdev.2015.02.002.
[2] To WM, Lee PKC, Yu BTW. Sustainability assessment of an urban rail system – The case of Hong Kong. J Clean Prod 2020:253. https://doi.org/10.1016/j.jclepro.2020.119961.
[3] Senaratne S, Mirza O, Dekruif T, Camille C. Life cycle cost analysis of alternative railway track support material: A case study of the Sydney harbour bridge. J Clean Prod 2020:276. https://doi.org/10.1016/j.jclepro.2020.124258.
[4] G. de E. Ministerio de Fomento, Informe anual del Observatorio del Transporte y la Logistica en España, n.d.
[5] G. de E. Ministerio de Fomento, Informe de la Comisión técnico-cientifica para el estudio de mejoras en el sector ferroviario, n.d.
[6] E. Union, Transport emissions, (n.d.). https://ec.europa.eu/clima/eu-action/transport-emissions_es (accessed April 21, 2022).
[7] Bosso N, Gugliotta A, Zampieri N. A Comprehensive Strategy to Estimate Track Condition and its Evolution. Int J Railw Technol 2012;1:1–19. https://doi.org/10.4203/ijrt.1.2.1.
[8] Nguyen K, Goicolea JM, Galbadon F. Dynamic effect of high speed railway traffic loads on the ballast track settlement. Congr Métodos Numéricos Em Eng 2011.
[9] Indraratna B, Nimbalkar S, Rujikiatkamjorn C. Modernisation of Rail Tracks for Higher Speeds and Greater Freight. Int J Railw Technol 2013;2:1–20. https://doi.org/10.4203/ijrt.2.3.1.
[10] Fortunato E, Paixão A, Calçada R. Railway Track Transition Zones: Design, Construction, Monitoring and Numerical Modelling. Int J Railw Technol 2013;2:33–58. https://doi.org/10.4203/ijrt.2.4.3.
[11] Sainz-Aja J, Pombo J, Tholken D, Carrascal I, Polanco J, Ferreño D, Casado J, Diego S, Perez A, Filho JEAA, Esen A, Cebasek TM, Laghrouche O, Woodward P. Dynamic calibration of slab track models for railway applications using full-scale testing. Comput Struct 2020;228:106180. https://doi.org/10.1016/j.compstruc.2019.106180.
[12] Mezher SB, Connolly DP, Woodward PK, Laghrouche O, Pombo J, Costa PA. Railway critical velocity – Analytical prediction and analysis. Transp Geotech 2016;6:84–96. https://doi.org/10.1016/j.trgeo.2015.09.002.
[13] Momoya Y, Nakamura T, Fuchigami S, Takahashi T. Improvement of Degraded Ballasted Track to Reduce Maintenance Work. Int J Railw Technol 2016;5:31–54. https://doi.org/10.4203/ijrt.5.3.2.
[14] Sañudo R, Pombo J, Ricci S, Miranda M. The importance of sleepers spacing in railways. Constr Build Mater 2021;300:124326. https://doi.org/10.1016/j.conbuildmat.2021.124326.
[15] Woodward PK, Laghrouche O, Mezher SB, Connolly DP. Application of Coupled Train-Track Modelling of Critical Speeds for High-Speed Trains using Three-Dimensional Non-Linear Finite Elements. Int J Railw Technol 2015;4:1–35. https://doi.org/10.4203/ijrt.4.3.1.
[16] Thölken D, Abdalla Filho JE, Pombo J, Sainz-Aja J, Carrascal I, Polanco J, Esen A, Laghrouche O, Woodward P. Three-dimensional modelling of slab-track systems based on dynamic experimental tests. Transp Geotech 2021:31. https://doi.org/10.1016/j.trgeo.2021.100663.
[17] Kaewunruen S, Remennikov AM. Laboratory Measurements of Dynamic Properties of Rail Pads under Incremental Preload, in: 19th Australas. In: Conf. Mech. Struct. Mater. Christchurch, New Zealand: Taylor & Francis; 2007. p. 319–24.
[18] Sainz-Aja JA, Carrascal IA, Ferreño D, Pombo J, Casado JA, Diego S. Influence of the operational conditions on static and dynamic stiffness of rail pads. Mech Mater 2020;148.
[19] Ferreño D, Sainz-Aja JA, Carrascal IA, Cuartas M, Pombo J, Casado JA, Diego S. Prediction of mechanical properties of rail pads under in-service conditions through machine learning algorithms. Adv Eng Softw 2021:151. https://doi.org/10.1016/j.advengsoft.2020.102927.
[20] Carrascal IA, Casado JA, Diego S, Sainz-Aja JA, Ferreño D, Barrientos A, García D. Influence of the Testing Procedure on the Value of the Impact Attenuation of Rail Fastening Systems: an Experimental Study. Exp Tech 2022;46:167–78. https://doi.org/10.1007/s40799-021-00468-y.
[21] Carrascal IAIAIA, Pérez A, Casado JA, Diego S, Polanco JA, Ferreño D, Martín JJJJJ. Experimental study of metal cushion pads for high speed railways. Constr Build Mater 2018;182:273–83. https://doi.org/10.1016/j.conbuildmat.2018.06.134.
[22] Dahlberg TLE. On the use of under-sleeper pads in tracks with varying track stiffness. In: Proc. - 9th Int. Heavy Haul Conf. "Heavy Haul Innov. Dev.; 2009.
[23] Pita AL, Teixeira PF, Robuste F. High speed and track deterioration: The role of vertical stiffness of the track. Proc Inst Mech Eng Part F J Rail Rapid Transit 2004;218:31–40. https://doi.org/10.1243/095440904322804411.
[24] Hou B, Wang D, Wang B, Chen X, Pombo J. Vibration Reduction in Ballasted Track Using Ballast Mat: Numerical and Experimental Evaluation by Wheelset Drop Test. Appl Sci 2022;12:1844. https://doi.org/10.3390/app12041844.
[25] Sol-Sánchez M, Moreno-Navarro F, Rubio-Gámez MC. The use of elastic elements in railway tracks: A state of the art review. Constr Build Mater 2015;75:293–305. https://doi.org/10.1016/j.conbuildmat.2014.11.027.
[26] Ferreño D, Casado JA, Carrascal IA, Diego S, Ruiz E, Saiz M, Sainz-Aja JA, Cimentada AI. Experimental and finite element fatigue assessment of the spring clip of the SKL-1 railway fastening system. Eng Struct 2019:188. https://doi.org/10.1016/j.engstruct.2019.03.053.
[27] Varandas JN, Paixão A, Fortunato E, Hölscher P, Calçada R. Numerical Modelling of Railway Bridge Approaches: Influence of Soil Non-Linearity. Int J Railw Technol 2014;3:73–95. https://doi.org/10.4203/ijrt.3.4.4.
[28] Sainz-Aja J, Carrascal I, Polanco J, Thomas C, Sosa I, Casado J, Diego S. Self-compacting recycled aggregate concrete using out-of-service railway superstructure wastes. J Clean Prod 2019;230:945–55. https://doi.org/10.1016/j.jclepro.2019.04.386.
[29] Ramos A, Gomes Correia A, Calçada R, Alves Costa P, Esen A, Woodward PK, Connolly DP, Laghrouche O. Influence of track foundation on the performance of ballast and concrete slab tracks under cyclic loading: Physical modelling and numerical model calibration. Constr Build Mater 2021;277:122245. https://doi.org/10.1016/j.conbuildmat.2021.122245.
[30] Sainz-Aja J, Carrascal I, Thomas C. Fatigue failure micromechanisms in recycled aggregate mortar by μCT analysis. J Build Eng 2020;28:101027. https://doi.org/10.1016/j.jobe.2019.101027.
[31] Antunes P, Magalhães H, Ambrósio J, Pombo J, Costa J. A co-simulation approach to the wheel–rail contact with flexible railway track. Multibody Syst Dyn 2019:45. https://doi.org/10.1007/s11044-018-09646-0.
[32] Costa J, Antunes P, Magalhães H, Pombo J, Ambrósio J. A novel methodology to automatically include general track flexibility in railway vehicle dynamic analyses. Proc Inst Mech Eng Part F J Rail Rapid Transit 2020:095440972094542. https://doi.org/10.1177/0954409720945420.
[33] Pombo J, Almeida T, Magalhães H, Antunes P, Ambrósio J. Finite Element Methodology for Flexible Track Models in Railway Dynamics Applications. Int J Veh Struct Syst 2013;5. https://doi.org/10.4273/ijvss.5.2.01.
[34] Costa J, Antunes P, Magalhães H, Pombo J, Ambrósio J. A Finite Element Methodology to Model Flexible Tracks with Arbitrary Geometry for Railway Dynamics Applications. Comput Struct 2021.

[35] Muñoz S, Aceituno JF, Urda P, Escalona JL. Multibody model of railway vehicles with weakly coupled vertical and lateral dynamics. Mech Syst Signal Process 2019; 115:570–92. https://doi.org/10.1016/j.ymssp.2018.06.019.

[36] Pombo J, Ambrósio J, Silva M. A new wheel–rail contact model for railway dynamics. Veh Syst Dyn 2007;45:165–89. https://doi.org/10.1080/00423110600996017.

[37] Marques F, Magalhães H, Pombo J, Ambrósio J, Flores P. A three-dimensional approach for contact detection between realistic wheel and rail surfaces for improved railway dynamic analysis. Mech Mach Theory 2020;149:103825. https://doi.org/10.1016/j.mechmachtheory.2020.103825.

[38] Sichani MS, Enblom R, Berg M. Non-Elliptic Wheel-Rail Contact Modelling in Vehicle Dynamics Simulation. Int J Railw Technol 2014;3:77–96. https://doi.org/10.4203/ijrt.3.3.5.

[39] Pombo J, Ambrósio J. Application of a wheel–rail contact model to railway dynamics in small radius curved tracks. Multibody Syst Dyn 2008;19:91–114. https://doi.org/10.1007/s11044-007-9094-y.

[40] Marques F, Magalhães H, Liu B, Pombo J, Flores P, Ambrósio J, Piotrowski J, Bruni S. On the generation of enhanced lookup tables for wheel-rail contact models. Wear 2019;434–435:202993. https://doi.org/10.1016/j.wear.2019.202993.

[41] Alonso A, Guiral A, Gimenez JG. Wheel Rail Contact: Theoretical and Experimental Analysis. Int J Railw Technol 2013;2:15–32. https://doi.org/10.4203/ijrt.2.4.2.

[42] Magalhães H, Marques F, Liu B, Antunes P, Pombo J, Flores P, Ambrósio J, Piotrowski J, Bruni S. Implementation of a non-Hertzian contact model for railway dynamic application. Multibody Syst Dyn 2019. https://doi.org/10.1007/s11044-019-09688-y.

[43] Liu Y, Montenegro P, Gu Q, Guo W, Calçada R, Pombo J. A Practical Three-Dimensional Wheel-Rail Interaction Element for Dynamic Response Analysis of Vehicle-Track Systems. Comput Struct 2021.

[44] Marques F, Magalhães H, Pombo J, Ambrósio J, Flores P. Utilization of Non-Conformal Wheel Surfaces for Railway Dynamics. Mech Mach Sci 2019:3291–300. https://doi.org/10.1007/978-3-030-20131-9_325.

[45] Vollebregt EAH, Steenbergen MJMM. A Methodology for Assessing Track Irregularities with respect to Rail Damage. Int J Railw Technol 2015;4:85–105. https://doi.org/10.4203/ijrt.4.4.5.

[46] Pombo J, Ambrósio J. An alternative method to include track irregularities in railway vehicle dynamic analyses. Nonlinear Dyn 2012;68:161–76. https://doi.org/10.1007/s11071-011-0212-2.

[47] Hsu SS, Fagan N. Improving Switches and Crossings Performance and Reliability. Int J Railw Technol 2016;5:79–93. https://doi.org/10.4203/ijrt.5.3.4.

[48] Coleman I, Kassa E, Smith R. Wheel-Rail Contact Modelling within Switches and Crossings. Int J Railw Technol 2012;1:45–66. https://doi.org/10.4203/ijrt.1.2.3.

[49] Hölscher P. The Dynamics of Foundations for High Speed Lines on Soft Soils. Int J Railw Technol 2012;1:147–66. https://doi.org/10.4203/ijrt.1.1.7.

[50] Sañudo R, Markine V, Pombo J. Study on Different Solutions to Reduce the Dynamic Impacts in Transition Zones for High-Speed Rail. J Theor Appl Vib Acoust 2017;3:199–222. https://doi.org/10.22064/tava.2018.80091.1095.

[51] Kuka N, Ariaudo C, Verardi R, Pombo J. Impact of rail infrastructure maintenance conditions on the vehicle-track interaction loads. Proc Inst Mech Eng Part C J Mech Eng Sci 2020:095440622096214. https://doi.org/10.1177/0954406220962144.

[52] Iwnicki SD, Bevan AJ. Damage to Railway Wheels and Rails: A Review of the Causes, Prediction Methods, Reduction and Allocation of Costs. Int J Railw Technol 2012;1:121–46. https://doi.org/10.4203/ijrt.1.1.6.

[53] Pombo J. Application of a Computational Tool to Study the Influence of Worn Wheels on Railway Vehicle Dynamics. J Softw Eng Appl 2012;05:51–61. https://doi.org/10.4236/jsea.2012.52009.

[54] Stichel S, Jönsson P-A, Casanueva C, Hossein Nia S. Modelling and Simulation of Freight Wagon with Special attention to the Prediction of Track Damage. Int J Railw Technol 2014;3:1–36. https://doi.org/10.4203/ijrt.3.1.1.

[55] Kuka N, Verardi R, Ariaudo C, Pombo J. Impact of maintenance conditions of vehicle components on the vehicle–track interaction loads. Proc Inst Mech Eng Part C J Mech Eng Sci 2018;232:2626–41. https://doi.org/10.1177/0954406217722803.

[56] Zhu S, Cai C, Luo Z, Liao Z. A frequency and amplitude dependent model of rail pads for the dynamic analysis of train-track interaction. Sci China Technol Sci 2015;58:191–201. https://doi.org/10.1007/s11431-014-5686-y.

[57] Fenander Å. Frequency dependent stiffness and damping of railpads. Proc Inst Mech Eng Part F J Rail Rapid Transit 1997;211:51–62. https://doi.org/10.1243/0954409971530897.

[58] Wei K, Wang F, Wang P, Liu ZX, Zhang P. Effect of temperature- and frequency-dependent dynamic properties of rail pads on high-speed vehicle–track coupled vibrations. Veh Syst Dyn 2017;55:351–70. https://doi.org/10.1080/00423114.2016.1267371.

[59] Wei K, Zhang P, Wang P, Xiao J, Luo Z. The Influence of Amplitude- and Frequency-Dependent Stiffness of Rail Pads on the Random Vibration of a Vehicle-Track Coupled System. Shock Vib 2016;(2016):1–10. https://doi.org/10.1155/2016/7674124.

[60] Wei K, Zhao Z, Ren J, Ou L, Wang P. High-speed vehicle–slab track coupled vibration analysis of the viscoelastic-plastic dynamic properties of rail pads under different preloads and temperatures. Veh Syst Dyn 2019:3114. https://doi.org/10.1080/00423114.2019.1673444.

[61] Kiani J, Camp C, Pezeshk S. On the application of machine learning techniques to derive seismic fragility curves 2019;218:108–22.

[62] Kawamura K, Miyamoto A. Condition state evaluation of existing reinforced concrete bridges using neuro-fuzzy hybrid system. Comput Struct 2003;81:1931–40. https://doi.org/10.1016/S0045-7949(03)00213-X.

[63] Basudhar A, Missoum S. Adaptive explicit decision functions for probabilistic design and optimization using support vector machines. Comput Struct 2008;86:1904–17. https://doi.org/10.1016/J.COMPSTRUC.2008.02.008.

[64] Hénon M. The Monte Carlo method. Int. Astron. Union Colloq. Cambridge University Press; 1971. p. 151–67.

[65] Rubinstein RY, Kroese DP. Simulation and the Monte Carlo method. John Wiley & Sons; 2016.

[66] Metropolis N, Ulam S. The monte carlo method. J Am Stat Assoc 1949;44:335–41.

[67] T. Benz, Small-strain stiffness of soils and its numerical consequences, (2007).

[68] Uzielli M, Lacasse S, Nadim F, Phoon KK. Soil variability analysis for geotechnical practice. Charact Eng Prop Nat Soils 2006;3:1653–752.

[69] Cherubini C, Christian JT, Baecher GB, Failmezger RA, Focht JA, Focht JA, Koutsoftas DC, Ladd CC, Da Re G, Li KS, Lam J, Moriwaki Y, Barneich JA, Schmertmann JH, Duncan JM. Factor of Safety and Reliability in Geotechnical Engineering. J Geotech Geoenviron Eng 2001;127:700–21. https://doi.org/10.1061/(ASCE)1090-0241(2001)127:8(700).

[70] Phoon K-K, Kulhawy FH. Characterization of geotechnical variability. Can Geotech J 1999;36:612–24.

[71] CEN, EN 1992-2 ***Eurocode 2: Design of conrete structures. Concrete bridges. Design and detailing curves***. 2010.

[72] Kottegoda NT, Rosso R. Applied statistics for civil and environmental engineers. MA: Blackwell Malden; 2008.

[73] Wikipedia, EPDM rubber, (n.d.). http://web.archive.org/web/20200811125540/https://en.wikipedia.org/wiki/EPDM_rubber.

[74] B.P. Federation, Thermoplastic Elastomers TPE, (n.d.). /web/20200811130117/https://www.bpf.co.uk/plastipedia/polymers/thermoplastic_elastomers.aspx.

[75] British plastic Federation, Ethylene Vinyl Acetate EVA, (n.d.). http://web.archive.org/web/20200811130052/https://www.bpf.co.uk/plastipedia/polymers/eva.aspx.

[76] Magalhães H, Madeira JFA, Ambrósio J, Pombo J. Railway vehicle performance optimisation using virtual homologation. Veh Syst Dyn 2016;54:1177–207. https://doi.org/10.1080/00423114.2016.1196821.

[77] Magalhães H, Ambrósio J, Pombo J. Railway Vehicle Modelling for the Vehicle–Track Interaction Compatibility Analysis. Proc Inst Mech Eng Part K J Multi-body Dyn 2016;230:251–67. https://doi.org/10.1177/1464419315608275.

[78] Magalhães H, Pombo J, Ambrósio J, Madeira JFA. Rail vehicle design optimization for operation in a mountainous railway track. Innov Infrastruct Solut 2017;2. https://doi.org/10.1007/s41062-017-0088-1.

[79] Magalhaes H, Marques F, Antunes P, Flores P, Pombo J, Ambrósio J, Qazi A, Sebes M, Yin H, Bezin Y. Wheel-rail contact models in the presence of switches and crossings. Veh Syst Dyn 2022:1–33. https://doi.org/10.1080/00423114.2022.2045026.

[80] Marolt Čebašek T, Esen AF, Woodward PK, Laghrouche O, Connolly DP. Full scale laboratory testing of ballast and concrete slab tracks under phased cyclic loading. Transp Geotech 2018;17:33–40. https://doi.org/10.1016/J.TRGEO.2018.08.003.

[81] Base de datos Meteorologica, (n.d.). /web/20200812123028/https://datosclima.es/Aemethistorico/Tempestad.php.

[82] Moscow temperature database, (2018). https://www.meteoblue.com/en/weather/archive/export/moscow_russia_524901.

[83] CEN, EN 13674-1. Railway applications - Track - Rail - Part 1: Vignole railway rails 46 kg/m and above. 2012.

[84] Cramer JS. The origins of logistic regression. 2002. https://doi.org/10.2139/ssrn.360300.

[85] Nilsson NJ. Learning Machines: Foundations of Trainable Pattern-Classifying Systems. 1965.

[86] Yadav P. Decision Tree in Machine Learning, Towar. Data Sci 2018.

[87] Ferreño D, Serrano M, Kirk M, Sainz-aja JA. Prediction of the Transition-Temperature Shift Using Machine Learning Algorithms and the Plotter Database. Metals (Basel) 2022;12. https://doi.org/10.3390/met12020186.

[88] Hebb D. The Organization of Behavior. New York: Wiley; 1949.

[89] Permutation Importance vs Random Forest Feature Importance (MDI). Scikit-Learn 0.22.Dev0. 2019.

[90] Feature importances with forests of trees, Scikit-Learn v0.21.3. (n.d.).